Pechini Synthesis Method of Ho_2O_3 Nanoparticles and Their Harnessing for Extremely Sensitive Electrochemical Sensing of Diuron in Juice Samples; Theoretical insights into sensing principle

Aleksandar Mijajlović[1], Vesna Stanković[2*], Filip Vlahović[2], Miloš Ognjanović[3], Kurt Kalcher[4], Astrid Ortner[5], Dalibor Stanković[1]

[1]*Department of Analytical Chemistry, Faculty of Chemistry, University of Belgrade, Studentski trg 12-16, 11000 Belgrade, Serbia*
[2]*Department of Chemistry, Institute of Chemistry, Technology and Metallurgy, University of Belgrade, Njegoševa 12, 11000 Belgrade, Serbia*
[3]*Institute of Nuclear Sciences „Vinča", University of Belgrade, Mike Petrovića Alasa, 12-14, Belgrade, Serbia*
[4]*Analytical Chemistry, Institute of Chemistry, Karl-Franzens University, Universitaetsplatz I/I, 8010 Graz, Austria*
[5]*Department of Pharmaceutical Chemistry, Institute of Pharmaceutical Sciences, University of Graz, Schubertstraße 1, 8010, Graz, Austria*

Abstract

This study developed a new electrochemical sensor for diuron (DIU) detection using a carbon paste electrode (CPE) upgraded with Ho_2O_3 nanoparticles. The Pechini method was used to synthesize Ho_2O_3 nanoparticles. The nanostructure properties of the material were confirmed using X-ray powder diffraction (XRPD), attenuated total reflectance (ATR) - Fourier transform infrared (FTIR) spectroscopy and scanning electron microscopy (SEM). The material electrocatalytic features were investigated using cyclic voltammetry (CV) and electrochemical impedance spectroscopy (EIS). An analytical method for identifying and measuring DIU was established using square wave voltammetry (SWV). The proposed sensor exhibited a remarkable response to DIU, displaying a broad linear range (0.25 - 200 μM) and a detection limit of 0.03 μM. Its minimal influence from potential interfering substances confirmed the method's selectivity. When detecting DIU in water and juice samples, the CPE/Ho_2O_3 sensor showed good recovery results. The conventional UV-Vis detection method validated the sensor efficacy.

Keywords: holmium oxide nanoparticles; diuron; pesticide; carbon paste electrode; DFT; Pechini synthesis

Introduction

Embracing development, modernization, and the expansion of food production is crucial in today's era. However, it is equally essential to understand and mitigate the potential impact on the environment and human health due to the use of numerous chemicals in this process. Many of these chemicals possess specific properties such as persistence, non-degradability, and potential toxicity to the living world.

Pesticides, including diuron, play a crucial role in enhancing agricultural productivity and improving the quality of agricultural products. They effectively manage and prevent the damage caused by agricultural pests and diseases, thereby ensuring a steady supply of food [1–3]. Diuron (N-(3,4-dichlorophenyl)-N,N-dimethylurea) is a widely used herbicide for crops such as citrus fruits, rice, cotton, soybeans, sugarcane, potato, wheat, tea, and coffee. Additionally, it is commonly applied along airport runways, railroads, and pipelines. Its primary purpose is to inhibit the Hill reaction in photosynthesis by decreasing the production of high-energy molecules, including adenosine triphosphate (ATP), which are used for various metabolic activities [4]. This substance poses a significant concern because it remains stable in water and soil and could harm the environment and living organisms. When absorbed by plant roots, it can move to the stem and leaves and inhibit photosynthesis. In humans, exposure to this substance can lead to the production of methemoglobin in the bloodstream, as well as abnormalities in the liver and spleen and disruptions in the release and transportation of natural hormones throughout the body [5]. Various techniques have been documented for effectively detecting DIU, including electrochemical sensors, capillary electrophoresis, gas chromatography, and liquid chromatography combined with mass spectrometry approaches [6–8]. Capillary electrophoresis provides excellent separation capabilities but often struggles to achieve the low detection limits needed to identify pesticide traces. In contrast, gas and liquid chromatography coupled with mass spectrometry are highly sensitive techniques capable of detecting very low concentrations of various analytes. However, these methods require expensive equipment and trained personnel. More affordable alternatives that offer both precision and accuracy include electrochemical methods and electrochemical sensors. The detection process in electrochemical sensors relies on electron transfer between the electrode surface and target molecules through redox reactions. Such reactions involve either the oxidation (electron loss) or reduction (electron gain) of the analyte at the electrode surface, effectively translating chemical data into measurable electrical signals, such as changes in current

or potential. The electrode surface is pivotal in this process, enabling direct analyte interaction and facilitating electron transfer. By modifying the electrode surface with chemical coatings or functionalized materials, both the sensor's selectivity and sensitivity can be significantly improved [9].

In the past years, there has been a surge in research interest in electrochemical sensors due to their exceptional stability, sensitivity, and selectivity, as well as their rapidity, affordability, scalability, and high consistency [10–14]. Particularly intriguing candidates for developing novel electrochemical sensors are rare earth elements due to their distinctive characteristics, including control structures, superior physical and chemical properties, and an unpaired electronic configuration consisting of 4f orbitals [15,16]. Rare earth elements also impart favorable optical and thermal properties and high conductivity [17,18]. Rare earth oxides have excellent electrical conductivity, allowing for efficient electron transfer between the analyte and the electrode surface. This property significantly boosts the sensor's sensitivity, enabling the detection of low analyte concentrations. Additionally, rare earth oxides have unique surface properties including high surface area and controllable surface chemistry, which allows customization of sensors surface to provide enhanced stability, increased binding sites for analytes, and improved biocompatibility [19].

The synthesis of REOs is based on applying hydrothermal, sol-gel, sonochemical methods, etc. The Pechini method entails the creation of a complex compound between metal cations and a molecule containing hydroxycarboxylic acid, followed by the polymerization of this compound with a polyhydroxy alcohol [20,21]. The Pechini approach, which is less expensive than other sol-gel techniques, results in the production of nanometer-sized powders after the calcination process. This method also offers a significant advantage in terms of reduced toxicity, providing a sense of reassurance and safety in the nanoparticle preparation process [17].

In this paper, for the first time, the modified variant of the Pechini process was used to synthesize holmium oxide nanoparticles (Ho_2O_3). The as-synthesized Ho_2O_3 nanoparticles were integrated with the carbon paste, thus forming the electrode material for developing a new electrochemical sensor (CPE/ Ho_2O_3). Adding Ho_2O_3 significantly enhanced the electrocatalytic activity and conductivity of the CPE in the proposed sensor, as confirmed by the EIS, CV, and SWV techniques. The prepared sensor was then used to develop a detection method for DIU. According

to the results, DIU is oxidized on the proposed electrode at a potential of about 0.8 V. Extensive theoretical calculations were performed to clarify the proposed DIU sensing mechanism, making this the first exploration of such a concept. Furthermore, an analytical method for identifying and measuring DIU was established using square wave voltammetry (SWV). The exceptional performance of the proposed approach, using CPE/Ho_2O_3 sensor, indicates its potential for detecting DIU in water, apple, and strawberry juice samples, thereby offering a promising solution for environmental and food safety monitoring.

Experimental section

Chemicals and instrumentation

Holmium (III) chloride hexahydrate ($HoCl_3$ x 6H2O), anhydrous citric acid, acrylic acid, hydroquinone, acetonitrile, sodium hydroxide (NaOH), potassium ferrocyanide ($K_4[Fe(CN)_6]$), potassium ferricyanide ($K_3[Fe(CN)_6]$), potassium chloride (KCl), and DIU were obtained from Sigma-Aldrich and directly used for the experimental investigations without purification. Graphite (powder, < 20 μm, synthetic) used for electrode preparation was obtained from Sigma Aldrich.

For electrochemical measurements (cyclic voltammetry, square wave voltammetry) the potentiostat/galvanostat Autolab, model PGSTAT302N (Metrohm, the Netherlands) was used. A classical three-electrode system was used. As working electrode, bare or modified CPE was used, while a platinum plate was used as a counter electrode and Ag/AgCl (3 M KCl) as a reference one. Electrochemical impedance spectroscopy (EIS) measurements were performed using a potentiostat/galvanostat CHI 760b (CH Instruments, Inc., Austin, Texas, USA). For all electrochemical measurements, Britton–Robinson buffer solution (BRBS) was used. This solution was prepared by mixing equimolar amounts of phosphoric, acetic, and boric acids (0.04 M) and NaOH solution (0.2 M) was used for tuning and obtaining the desired pH buffer values (from 3 to 11). A pH meter equipped with a universal glass electrode (Orion 1230, Thermo Fisher Scientific, Waltham, Massachusetts, USA) was used for all pH measurements. For the preparation of all solutions, double-distilled water was used.

The UV/VIS analysis was performed on Evolution 220 UV-Visible Spectrophotometer (Thermo Scientific).

A JEOL JSM-7001F scanning electron microscope (SEM) (JEOL, Japan) was used for detailed surface analysis of the Ho_2O_3 nanomaterial. The SEM was equipped with an Oxford Instruments (UK) X-MAX 80 energy-dispersive X-ray spectroscopy (EDS) system for elemental analysis. The X-MAX 80 EDS utilizes a large-area silicon drift detector (80 mm^2 active area).

A high-resolution X-ray powder diffraction (XRPD) technique (Smart Lab® diffractometer, Rigaku, Japan) was used to analyze the crystal structure of the dried Ho_2O_3 powder. The analysis employed Cu Kα radiation (wavelength of 1.5406 Å) generated at 40 kV and 30 mA. The data was collected between 15° and 65° degrees 2θ with a scan rate of 1° min^{-1}. Powdered sample was flattened with a silicon holder and analyzed by XRPD.

ATR-FTIR spectroscopy was employed in the mid-infrared region (4000-400 cm^{-1}) to investigate the surface chemistry of the particles. A Nicolet iS50 FT-IR spectrometer (Thermo Fisher Scientific, USA) equipped with a Smart iTR ATR accessory was used for the analysis. The powdered sample was pressed onto a diamond crystal plate using a swivel press to ensure good contact with the infrared light. Background spectra were collected from a clean diamond crystal and subtracted using OMNIC™ Specta Software.

Preparation of Ho_2O_3 nanoparticles

For the preparation of Ho_2O_3 nanoparticles, a slightly modified Pechini method, a widely recognized and efficient technique in materials science [22], was employed. This method involves the combination of citric acid (0.12 mol) and acrylic acid (0.10 mol) with 0.1% hydroquinone in a three-neck round-bottom flask with a thermometer and condenser. The mixture temperature was gradually raised to 120 – 170 °C, leading to the production of a high-viscosity polymer with a whitish, yellowish hue through esterification at around 120 °C and further polymerization at higher temperatures. The appropriate concentration of a Ho^{3+} solution was added to the polyester, in the required volume. The optimal molar ratio of CA: Ho (III), was 0.09. After this step, the stirring persisted for an additional hour. The overnight drying of the solutions at a low temperature of 150 °C produced solid resins with a high porosity. The resultant resins undergo pyrolysis at 450 °C for 4 hours in glazed alumina crucibles after being pulverized in an agate mortar. The pyrolysis product was then heated to 900°C for 4 hours while being exposed to air.

Preparation of carbon paste electrode (CPE) modified with Ho_2O_3

Modification of CPE was done by mixing 72 mg of graphite and 8 mg of Ho_2O_3 composite with 20 μL of paraffin oil in a mortar. After homogenizing the mixture, the substance was allowed overnight to absorb the paraffin oil and obtain a finely distributed particle size.

Bare CPE was modified using various concentrations of Ho_2O_3 against graphite (5, 10, 15%), and the current responses were examined. The best ratio of Ho_2O_3 against graphite was 10 % (data not shown), so this ratio was used for all examinations.

Preparation of the real sample

For testing the sensor's applicability for detecting DIU in real samples, tap water samples, apple and strawberry juice samples, purchased in a local market, were used. The ability of the proposed sensor to accurately detect DIU in different matrices was inspect using the UV-Vis method. The extraction of DIU was achieved using acetonitrile. Five milliliters of the samples were diluted with 20 ml of acetonitrile, and the extraction was carried out for 15 minutes. After this period, the solvent was evaporated, and the remaining residue were dissolved in the supporting electrolyte solution (BRBS, pH = 7). Samples prepared in this way are subjected to electrochemical and spectrophotometric analysis, in order to verify the application of the proposed method.

Computational details

In order to further investigate experimental foundlings and explain DIU oxidation mechanism, theoretical modeling was applied. The entirety of these results was derived using the Gaussian 09 [23] electronic structure program suite (Revision A.03) by using the Density Functional Theory (DFT) methodology [24,25]. The computational analyses were executed utilizing the dispersion-corrected M06-2X [26] density functional approximation in conjunction with the 6-311++G** [27] orbital basis set for all atoms and the integration grid of ultra-fine quality. To enhance calculation accuracy, the solvation effects of water have been included using the polarizable conductor continuum model (C-PCM) through the solvent cavity reaction field (SCRF) method [28]. Mentioned computational conditions were applied for full relaxation and optimization of all molecular species of interest.

Results and discussion

Morphological characterization

The material characterization is given in **Fig. 1**. Scanning electron microscopy (SEM) micrograph of holmium (III) oxide nanoparticles is shown in **Fig.1A**, where fine nanoparticles are observed held by a more complex structure of several microns in size. The corresponding SEM-EDX spectrum in **Fig. 1B** reveals the elemental composition of 81.3 Wt.% of Ho and 18.2 Wt.% of O. The remaining 0.5 Wt.% is most probably due to impurities during the synthesis. **Fig. 1C** shows the X-ray diffractogram of a Ho_2O_3 nanoparticles. The XRPD analysis determined that the sample crystallizes in a single phase without any unwanted impurities or phases. Ho_2O_3 in this sample crystallizes in a body-centered cubic (bcc) structure with $Ia\bar{3}$ (No. 206) space group symmetry [29]. The average crystallite size of 26 ± 5 nm was determined using the Scherer equation. As a reference, a standard diffractogram of Ho_2O_3 (PDF #2101512) is given at the bottom of **Fig. 1C**. **Fig. 1D** displays the ATR-FTIR spectrum on which only two characteristic metal-oxygen vibrations are observed at 440 cm^{-1} and 555 cm^{-1} [30].

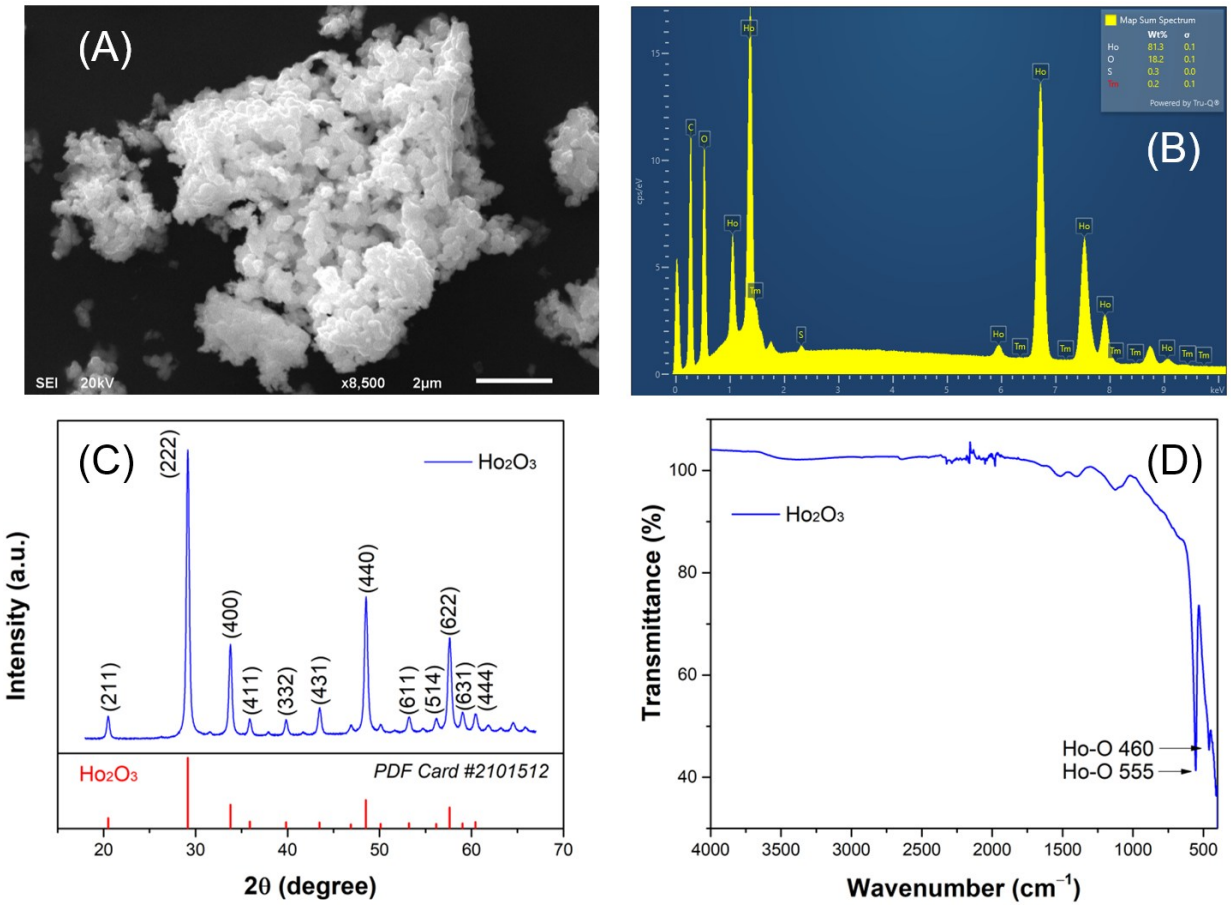

Fig. 1. A) Scanning electron microscopy of Ho_2O_3 nanoparticles; B) Corresponding SEM-EDX data of Ho_2O_3; C) X-ray diffractogram and D) ATR-FTIR spectrum of Ho_2O_3 nanoparticles.

Electrochemical characterization

Electrochemical impedance spectroscopy (EIS) is an important method for analyzing the characteristics of modified electrode surfaces and their ability to transmit electrons. Also, this technique provides kinetic and mechanistic data of electrochemical systems and is widely used in chemical sensing and biosensing. EIS measurements were performed in 0.1M KCl solution with 5 mM of $[Fe(CN)_6]^{3-/4-}$, at potential of 0 V and with the frequency ranging from 0.01 Hz to 100 kHz, using bare CPE and CPE/Ho_2O_3 (**Fig. 2A**). The impedance data were fitted to the Randles circuit depicted in the inset of **Fig. 2A**, where Rct represents charge transfer resistance, Rs represents electrolyte resistance, Zw represents Warburg impedance, and Cdl represents double-layer capacitance. The Rct value of the bare and modified electrodes depends on the size of the resultant semicircle since its diameter equals the Rct value, which represents the rate of electron transfer of the redox probe at the electrode/electrolyte interface. The Nyquist plot unveiled a significant difference between the bare CPE and the modified electrode. The bare CPE, with its larger semicircle diameter and higher Rct value (16 258 Ω), may have had fewer active sites and poor electron transferability. In contrast, the CPE enhanced with a nanosized Ho_2O_3, with its lower Rct value (12 058 Ω), presents a significant improvement regarding its ability to transmit electrons, likely due to a larger surface are and increased number of active sites. As a result of these findings, CPE/Ho_2O_3 demonstrates better electron transfer ability and lower charge transfer resistance, making it a promising material for the development of a new electrochemical sensor.

The catalytic activity of the proposed electrode was determined using the CV method in 5 mM $[Fe(CN)_6]^{3-/4-}$ and 0.1 M KCl as the supporting electrolyte (potential window -0.5 to 1.2 V, scan rate 50 mVs^{-1}). The CV analysis for both bare CPE and CPE/Ho_2O_3 are shown in **Fig. 2B**. When compared to the bare CPE, the modified electrode exhibits the pronounced redox peak current value in the observation of the CV findings. The larger surface area of the proposed Ho_2O_3 nanocomposite, which offered the great electrode/electrolyte interface for the accumulation of charges or ions and improved the fast electron transferability, was the primary cause of the higher redox current response of CPE/ Ho_2O_3 during electrocatalysis.

Influence of scan rate on electrode response was also studied in 0.1 M KCl solution containing 5 mM of $[Fe(CN)_6]^{3-/4-}$. **Fig. 2C** depicts the CV current response of CPE/ Ho_2O_3 toward redox couple, at various scanning rates, from 20 to 300 mVs^{-1}. With an increase in the scanning speed, an amplify in the current of the redox peaks is also noticeable. The dependence of the anodic (Ipa) and cathodic (Ipc) peak current values on the root of the scan rate is shown in the inset of **Fig. 2C** and can be described by the following linear equations: $Ipa = 9.31\times10^{-6} + 4.43\times10^{-6}$ ($R^2 = 0.992$) and $Ipc = -6.90\times10^{-6} - 1.31\times10^{-5}$ ($R^2 = 0.990$), respectively. These results indicate that the electrode processes on the CPE/Ho_2O_3 surface is diffusion controlled.

Randles−Sevcik equation $Ip = (2.69\times10^5)\times A\times n^{2/3}\times D^{1/2}\times C\times V^{1/2}$, where Ip stands for peak current, n for number of electrons (1), D is diffusion coefficient (7.6×10^{-5} cm^2 s^{-1}) and C is concentration, was used to calculate the electrochemical active surface area (EASA) of the redox process [31]. Based on the Randle's slope, the effective surface area of the CPE/ Ho_2O_3 was determined to be 0.026 cm^2.

The determined effective electrode surface area was used to further compute the surface coverages and surface concentrations of electroactive species on the reformed electrode using the Brown-Anson equation: $Ipa = (n^2\times F^2\times C\times A\times v)/4\times R\times T$; where F is the Faraday constant (96500 C mol^{-1}), n is the number of electrons transferred (n=1), A is the active electrode surface area (0.026 cm^2), R is the gas constant (8.314 $Jmol^{-1}K^{-1}$), Ipa is the oxidation current, C is surface concentration of the absorbed electroactive species and v is the scan rate (20 mVs^{-1}) [32]. From this equation, the surface concentrations of electroactive species of CPE/Ho_2O_3 was evaluated to be 1.36 x 10^{-7} mol dm^{-2}.

The proposed CPE/Ho_2O_3 demonstrated low Rct, large electrochemical active surface area, and effective surface concentration. Furthermore, the CPE/Ho_2O_3 obtained surface concentrations of electroactive species may help the rise in current density in the direction of the target. When taken as a whole, these elements increased electrocatalytic activity, which made it advantageous to employ as an electrochemical sensor for DIU detection. Comparison between bare CPE and CPE electrode modified with Ho_2O_3 toward DIU detection was accomplished by recording CV in BRBS, pH 7 with 100 µM of analyte (**Fig. 2D**). The obtained CV data showed that, in comparison to the bare CPE, the modified electrode had a preferable current response. When compared to bare CPE (Ipa = 0.562 µA), the anodic peak current was improved to Ipa = 1.54 µA when CPE/Ho_2O_3

electrode was used (Inset on **Fig. 2D**). This improvement confirms the positive influence of Ho_2O_3 nanoparticles on the electrode characteristics probably caused by unique characteristics of material itself, such as highly reactive species, dielectric properties, and quick charge transportation between the metal oxide surface and BRBS electrolyte to the DIU detection.

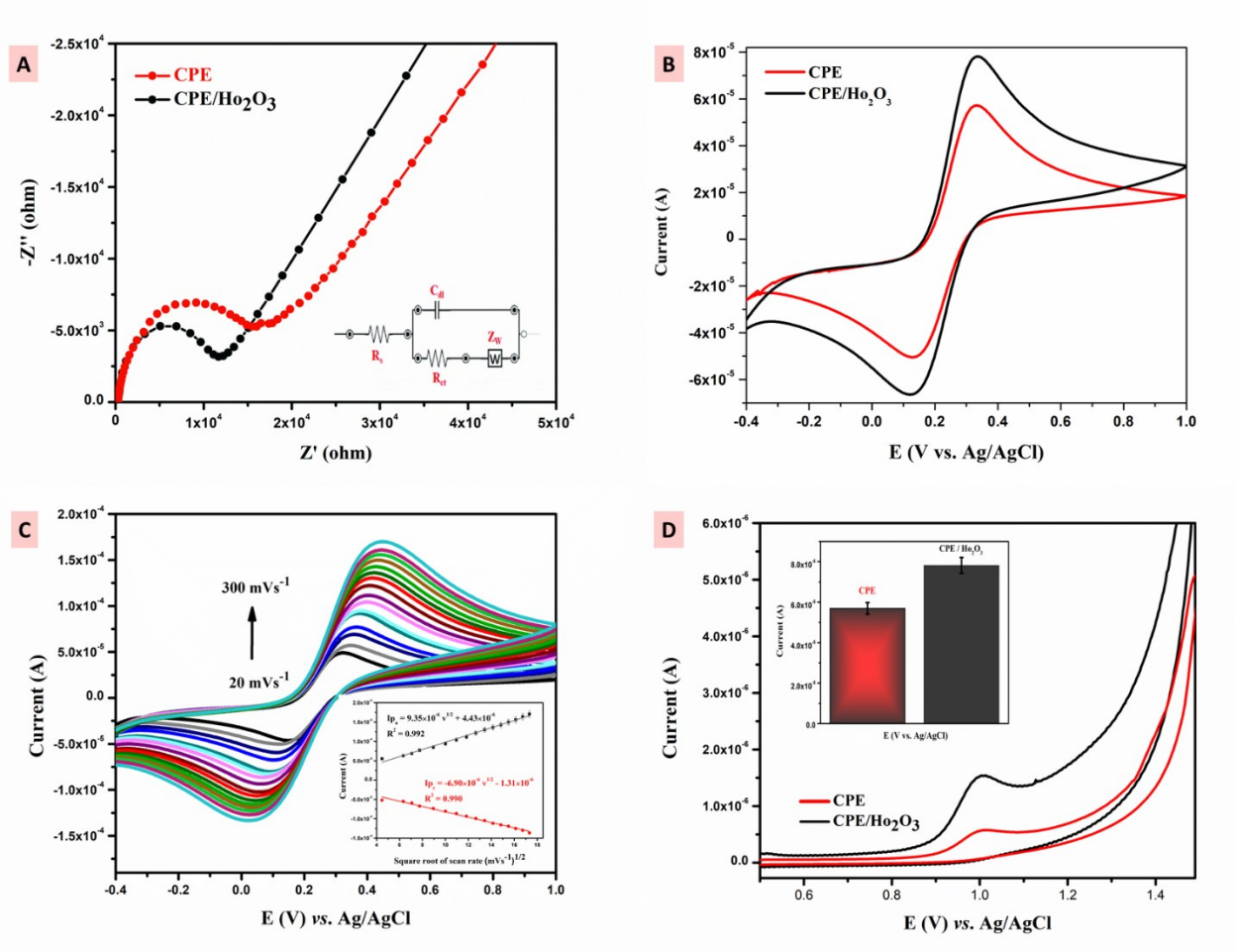

Fig. 2. A) Nyquist plot (Z′ *vs*. –Z″) and B) CVs for bare CPE and CPE/Ho_2O_3 C) Scan rate (20–300 mV s^{-1}) studies of CPE/ Ho_2O_3 in $[Fe(CN)_6]^{3-/4-}$ D) CVs of bare CPE and CPE/Ho_2O_3 in BRBS containing 100 µM of DIU

Electrochemical detection of DIU

The primary goal of this research was to create an electrochemical sensor based on merging of CPE and Ho_2O_3 that is capable of identifying DIU, precisely and with high accuracy. In order to investigate the nature of the electrode process taking place at the CPE/Ho_2O_3 electrode surface, the influence of scan rate on the oxidation peak current of 100 µM DIU was investigated using

cyclic voltammetry (**Fig. 3A**). The electrochemical kinetic mechanism was analyzed with the peak current versus square root of scan rate ($v^{1/2}$) plot (**Fig. 3B**), resulting in a linear equation of Ip (A) = 8.03×10^{-8} $v^{1/2}$ + 9.84×10^{-8} (R^2 = 0.994), indicating that the electrochemical mechanism of DIU oxidation at CPE/Ho_2O_3 is diffusion-controlled. Additionally, a correlation between the logarithm of scan rate (log v) and the logarithm of peak current (log Ip) was examined in order to confirm previous conclusion. It was discovered that this relationship also follows linear trend (**Fig. S1**), described by the equation: log Ipa (A) = 0.40 × log v – 6.85 (R^2=0.998) with a slope of 0.40, which is similar to the expected value of 0.5 for a diffusion-controlled process.

The supporting electrolyte's pH range may have a significant impact on electrode response toward DIU detection. The study of the influence of the pH value of the supporting electrolyte was performed using cyclic voltammetry (**Fig. 3C**), using 0.04 M BRBS with 100 µM of DIU at a scan rate of 50 mV s^{-1} in the pH range from 3 to 11. The highest DIU peak current was achieved when BRBS pH 7 was used. Additionally, the obtained result showed that the anodic peak potential (Epa) was shifted to the negative direction when the pH value increased, indicating that protons played a part in the electrochemical reaction of DIU. The linear relationship among pH and Epa has been shown in **Fig. 3D**. The linear regression equation and correlation coefficient that were found were: Epa= −0.055pH +1.28 and R^2=0.992, respectively. The obtained slope value was used in the Nernst equation:

$$Ep = -\left(\frac{0.0591\, m}{n}\right) pH + b$$

where m and n are the number of protons and electrons, respectively. Based on this equation, the m/n ratio was calculated to be 0.93 (close to 1) for DIU, suggests that an equal number of protons and electrons are involved in the electrochemical oxidation reaction of DIU at CPE/Ho_2O_3.

The proposed sensor, obtained by using carbon paste electrode (CPE) and Ho_2O_3 nanoparticles was used for the detection of DIU. Cyclic voltammetry indicated a diffusion-controlled mechanism for DIU oxidation, indicating equal participation of protons and electrons in the electrochemical reaction.

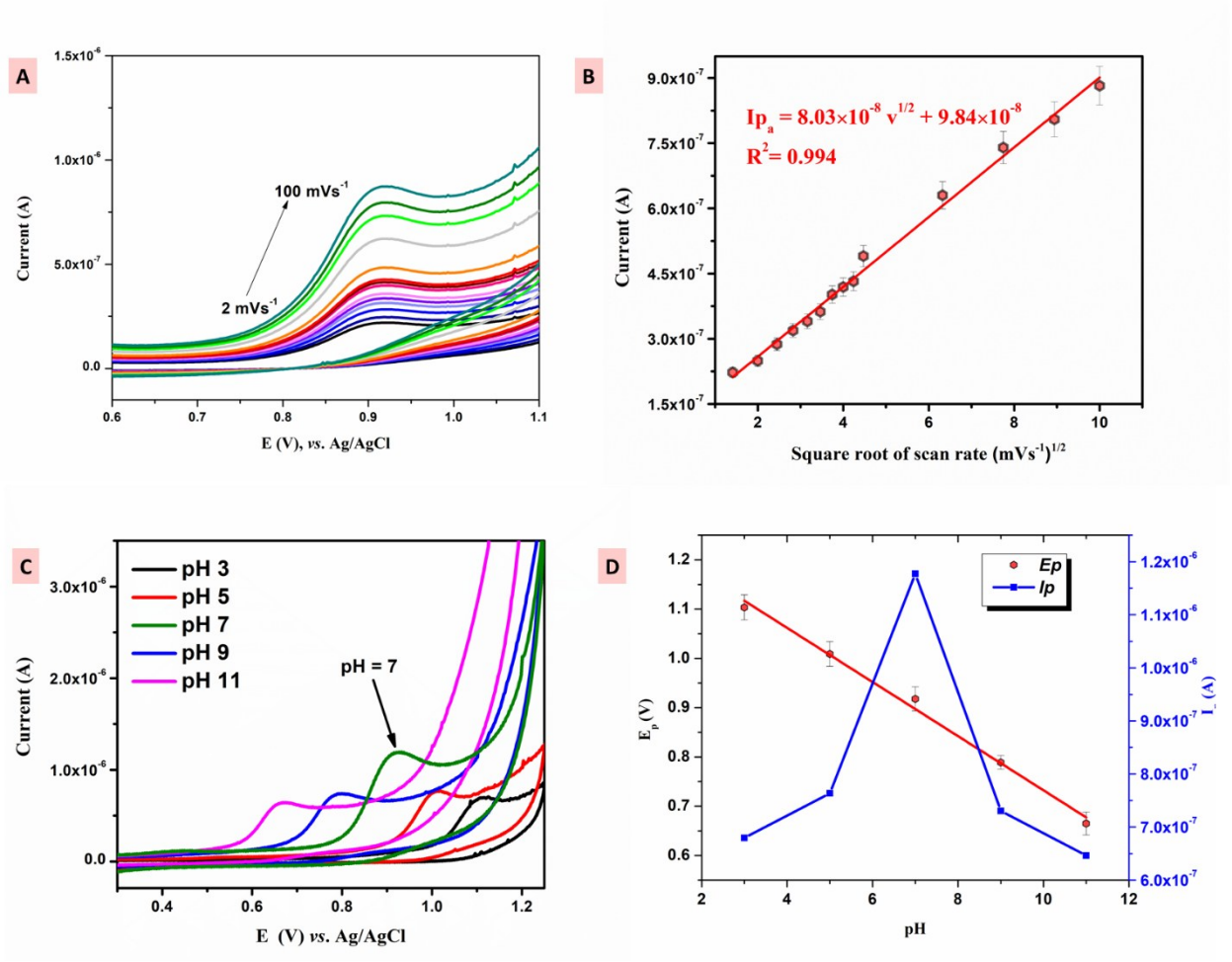

Fig. 3. A) The influence of scan rate on the oxidation peak current of 100 µM DIU B) Oxidation peak current *vs*. square root of scan rate ($v^{1/2}$) C) The impact of pH (3 – 11) on DIU electrode response (sweep rate of 50 mV s^{-1}) D) The effect of the pH value of supporting electrolyte on the oxidation peak Ep and Ip

Theoretical modeling of the experiment

To elucidate the underlying mechanisms governing the experimentally observed electrochemical behavior of DIU, a theoretical exploration of its oxidation process was undertaken. This commenced from the standpoint of the fully-relaxed ground-state electron density of DIU. **Fig. 4A and 4B** depict the molecular electrostatic potential (MEP) of DIU and oxidized $DIU^{+\cdot}$. This representation provides insight into the change in electron density (blue represents regions of decreased electron density, while red represents regions of increased electron density) after single-electron oxidation. Calculated MEPs clearly show that the region experiencing the most significant

change while going from DIU to $DIU^{+\cdot}$ includes the nitrogen atom N14 and the aromatic core of the system, suggesting that further (electro)chemical changes will occur in this part of the molecule. More specific information about reactive regions of the molecule can be drawn from the representation of the highest occupied molecular orbital (HOMO) and the lowest unoccupied molecular orbital (LUMO) of DIU, shown in **Fig. 4C**. Theoretically, an oxidation event is postulated to induce a significant alteration in the electron density, specifically within the HOMO orbital. The configuration and spatial distribution of the HOMO orbital, as depicted in **Fig. 4C**, underpin the assignment of the experimentally observed oxidation peak. This peak is attributed to the oxidation process occurring dominantly at the nitrogen atom N14 and the aromatic core of the DIU molecule.

The reactivity of the DIUs atomic sites was further investigated through atom-condensed Fukui index analysis. These indices reflect the susceptibility of an atomic site to gain or lose an electron, indicating its propensity to undergo nucleophilic (f^+), electrophilic (f^-), or radical attacks (f^0). Consequently, the calculated values provide insights into the tendency of specific sites to participate in these types of chemical interactions. **Fig. 4D** depicts the representation of the Fukui function for the nucleophilic attack, showing that the most reactive atomic centers within the molecule are N14 and C1. Following N14 and C1 in reactivity are the carbon atoms C5 and C6, which exhibit similar reactivity levels.

According to the obtained results, aromatic carbon atom C1 is especially relevant for further (electro)chemical transformations, such as the nucleophilic attack of a solvent molecule, leading to the substitution of the chlorine atom. Second, less pronounced reactive centers would be carbon atoms C5 and C6. Drawing from the theoretically obtained insights, two potential oxidation pathways can be proposed, as illustrated in **Fig. 4E**. The primary and more significant mechanism is hydrolytic dechlorination, while the secondary, less prominent mechanism is aromatic hydroxylation. Both mechanisms result in the formation of quinone imines (1-3). This hypothesis agrees with experimental and theoretical studies previously conducted in this domain [33]. This alignment reinforces the validity of the theoretical approach and provides a solid understanding of the underlying (electro)chemical process.

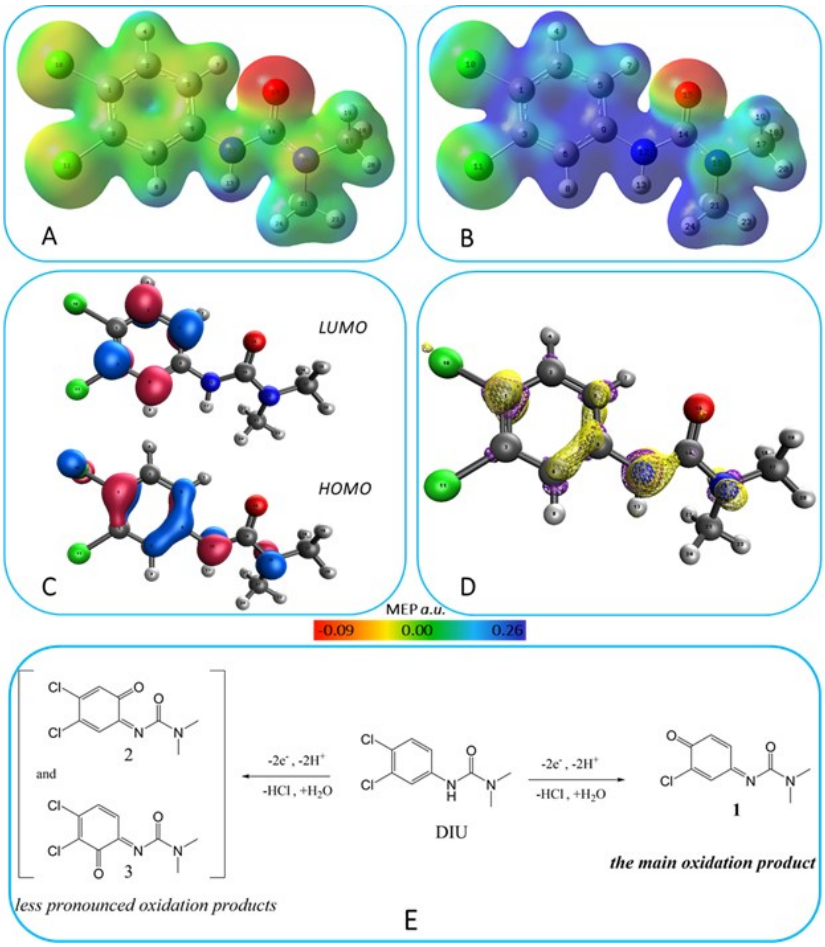

Fig. 4. A) MEP of DIU; B) HOMO and LUMO orbitals of DIU; C) MEP of $DIU^{+\cdot}$ D) Fukui function (f^+) representing the reactive centers of DIU prone to nucleophilic attack. E) Proposed oxidation mechanism of DIU at the surface of the electrode, determined by DFT.

Electrochemical determination of DIU by SWV analysis

The square wave voltammetry (SWV) was been utilized as method of choice for DIU determination, due to method qualities such as strong resolution, high sensitivity and lower background currents. Method parameters were optimized in order to get a wide calibration curve range with maximal slope (the best sensitivity) for the measurement of DIU. Keeping the other parameters fixed, each parameter was altered during the optimization process. The SWV was established using the target analyte's best-shaped peak and highest peak current, with a pulse amplitude of 20 mV, frequency of 25 Hz, and potential step of 5 mV. Under optimized conditions, SWV was recorded in 0.04 M BRBS (pH 7) after addition of DIU standard stock solution. From 0.25 to 200 µM, DIU concentrations increased continually, and DIU's oxidation peak current

response similarly climbed linearly (**Fig. 5A**). The existence of two linear ranges is observed (**Fig. 5B**), the first corresponds to concentrations from 0.25 to 20 µM, and the second to higher concentrations from 20 to 200 µM, described with following equations: Ipa = 5.56 $\times 10^{-8}$ C (µM) + 1.39 $\times 10^{-7}$ (R^2=0.990) and Ipa = 1.69$\times 10^{-9}$ C (µM) + 1.80 $\times 10^{-8}$ (R^2= 0.995), respectively. The existence of such a trend indicates the occurrence of analyte adsorption on the electrode, when higher analyte concentrations are used.

The results obtained confirmed the high electrocatalytic activity of CPE/Ho_2O_3 against DIU. The limit of detection (LOD) and limit of quantification (LOQ) were calculated from first calibration curve, using the equation LOD=3σ/s and LOQ = 10σ/s (where σ is the standard deviation of blank buffer solution (five repeated measurements) and s is slope value of corresponding curve). The calculated LOD and LOQ values were 0.03 µM and 0.1 µM. Additionally, sensitivity was also calculated as quotient of slope value and electroactive surface area and found to be 2.14 µA μM^{-1} cm^{-2}.

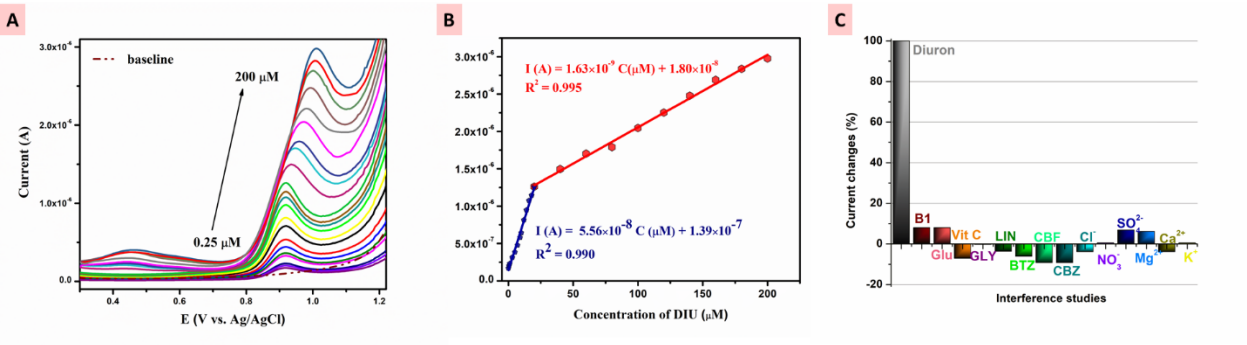

Fig. 5. A) The obtained SWV curves after every successive addition of DIU (concentration from 0.25 to 200 µM) B) The corresponding linear plot between the concentration of DIU versus anodic peak current (Ip_a) C) Current change (%) of 100 mM DIU oxidation peak in presence of interfering substances

The analytical parameters of the proposed method for diuron determination were compared with the CPE sensors reported so far and are shown in **Table S1**. The presented method has a wider operating range and a low detection limit, making the proposed material a promising candidate for further use in developing electrochemical sensors for pesticide detection.

Selectivity, Repeatability, Reproducibility, Storage Stability studies

The selectivity of the DIU sensor must be investigated since physiologically active molecules and other possibly concomitant inorganic substances may interfere with DIU detection in real-world applications. Thus, we used the proposed approach to investigate the selectivity of our CPE/Ho_2O_3 sensor by mixing 10 µM of DIU with 0.04 M BRBS (pH 7.0) and adding various possibly interfering ions and physiologically active compounds.

The 10 µM DU and 100-fold excess concentration of several common ionic interferences (K^+, Mg^{2+}, Ca^{2+}, NO_3^-, Cl^-, SO_4^{2-}) and biological interferences (glucose (Glu), vitamin B1, vitamin C) were used to test the selectivity of the proposed CPE/Ho_2O_3 sensor. Additionally, commonly used pesticides (carbofuran (CBF), carbendazim (CBZ), glyphosate (GLY), bentazone (BTZ) and linuron (LIN)) were also investigated as interfering substances. The results (**Fig. 5C**) showed that the DIU anodic current response was slightly impacted by these interfering species. Still, current changes were below 8.5 %, suggesting that proposed method possess good selectivity toward DIU detection.

Furthermore, investigations on repeatability and reproducibility were additionally looked at in order to determine the precision and readiness of DIU detection on modified CPE/Ho_2O_3 in 0.04 M BRBS. The modified electrode was tested six times in the presence of 100 µM of DIU in order to assess the repeatability of an emerging electrochemical sensor. The RSD was determined to be 5.65 %. The reproducibility studies were experimented with by using four different electrodes, modifying all these electrodes with the same electrolyte solution of 0.04 M BRBS on the same composite CPE/Ho_2O_3 by injecting 100 µM of DIU. The reproducibility was confirmed by observed RSD = 7.49%.

The long-term stability of the proposed electrode was also examined. Carbon paste modified with Ho_2O_3 nanoparticles was prepared and utilized for electrode fabrication on the same day, as well as after 5, 7, 15, and 30 days. These electrodes were employed to record solution containing 10 µM of DIU. The resulting relative standard deviation (RSD) value for these measurements was 3.93%, demonstrating excellent long-term stability of the CPE/Ho_2O_3 electrode.

Practical application study

The SWV investigation looked into the practical utility of our suggested CPE/Ho_2O_3 sensor. The DIU content in the strawberry juice, apple juice, and tap water samples was estimated using the

CPE/Ho_2O_3 sensor and proposed SWV method. UV-Vis spectrometry was used as validation method.

All samples were prepared by extraction method with acetonitrile. Firstly, voltammograms were recorded for all samples using proposed sensor. Since the presence of DIU was not detected, all samples were spiked with known DIU concentration, in order to check the possibility of sensor practical application. Three different concentrations of DIU (5, 10 and 20 µM) were added to each sample. Based on the obtained voltammograms (**Fig. 6A-C**), peak current intensities and calibration curves, the DIU concentration was determined, and the results were compared with the added values, on the basis of which the recovery values were estimated (**Table S2**). For additional confirmation of method accuracy, UV-Vis spectrometry was used for DIU determination in samples (**Fig. 6D-F**). The results for DIU determination obtained with CPE/Ho_2O_3 sensor largely match the results obtained with the UV-Vis validation method, which confirms the accuracy of the proposed approach (**Table S2**).

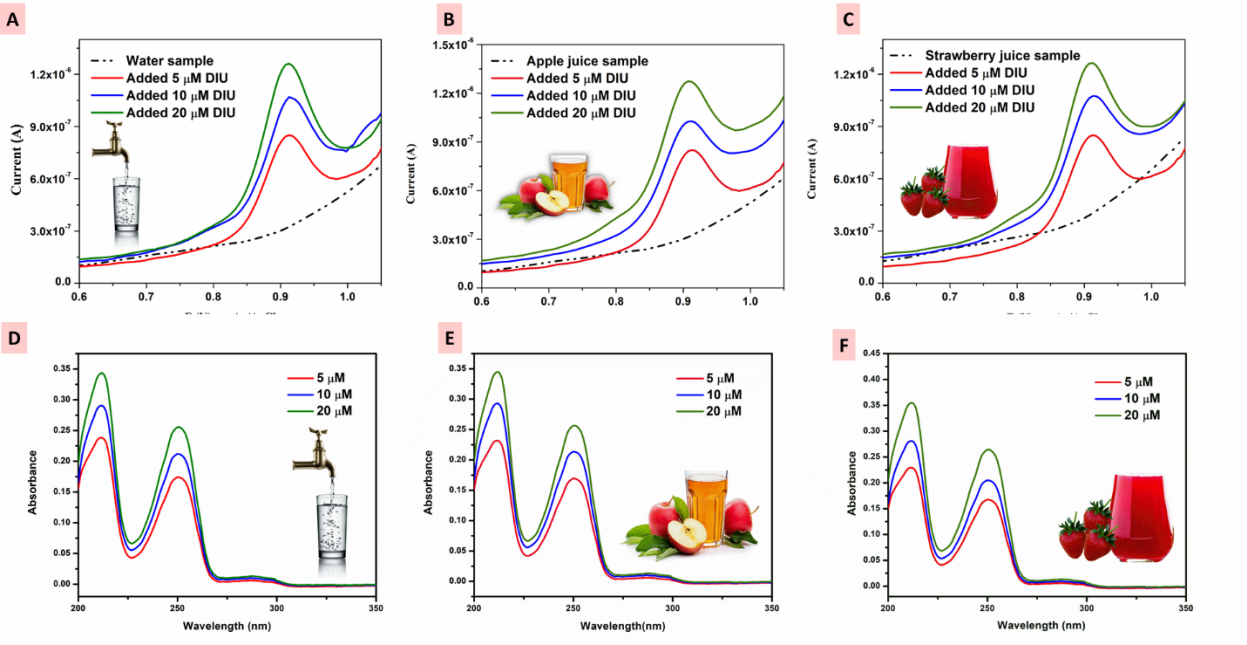

Figure 6. SWV current response for DIU detection in tap water (A), apple (B) and strawberry (C) juice samples at CPE/Ho_2O_3 electrode. UV-Vis analysis of DIU in tap water (D), apple (E) and strawberry (F) juice samples

Conclusion

The Ho_2O_3 nanoparticles were synthesized using the Pechini technique for the first time. The CPE electrode was integrated with the synthesized material to provide a novel electrochemical sensor for detecting pesticide diuron. An electrochemical approach was established, thanks to the inherent features of the working electrode. This method exhibits adequate analytical parameters, including a broad linear range, high sensitivity, and a low detection limit. In addition, most possible interfering substances do not impact the oxidation peak of DU, demonstrating a significant level of selectivity in the method. The method's achievement of a low detection limit (LOD) of 0.03 μM makes it a desirable contender for wider use.

Furthermore, the feasibility of the suggested sensor was validated by accurately measuring the DU concentration in real-life samples. Due to these factors, the new technique may be commercially used for efficient real-time monitoring of this herbicide in various matrices, offering a cost-effective alternative to current methods. The experimental findings reported here demonstrate that a CPE/Ho_2O_3 sensor has the potential to replace costly chromatographic approaches and provide a very sensitive method for monitoring herbicides.

Author contributions

Aleksandar Mijajlović: Investigation; Methodology; Writing - original draft. **Vesna Stanković**: Methodology; Validation; Visualization; Writing - original draft. **Filip Vlahović**: Writing - original draft; Formal analysis; Validation. **Miloš Ognjanović**: Writing - original draft; Methodology; Data curation; **Kurt Kalcher**: Conceptualization; Supervision; **Astrid Ortner**: Conceptualization; Supervision; **Dalibor Stanković**: Conceptualization; Supervision;

Declaration of Competing Interest

The authors declare that they have no known competing financial interests or personal relationships that could have appeared to influence the work reported in this paper.

Acknowledgments

This research has been financially supported by the Ministry of Science, Technological Development and Innovation of Republic of Serbia (Contract No: 451-03-66/2024-03/200026 and 451-03-66/2024-03/200168), CEEPUS network (CIII-CZ-0212-2425) and by the European Union,

MOBILES (Monitoring and detection of biotic and abiotic pollutants by electronic, plants and microorganisms based sensors), Grant Agreement 101135402, https://doi.org/10.3030/101135402

References

1. Berrada, H.; Font, G.; Moltó, J.C. Determination of Urea Pesticide Residues in Vegetable, Soil, and Water Samples. *Critical Reviews in Analytical Chemistry* **2003**, *33*, 19–41, doi:10.1080/713609152.
2. Songa, E.A.; Okonkwo, J.O. Recent Approaches to Improving Selectivity and Sensitivity of Enzyme-Based Biosensors for Organophosphorus Pesticides: A Review. *Talanta* **2016**, *155*, 289–304, doi:10.1016/j.talanta.2016.04.046.
3. Yan, X.; Li, H.; Su, X. Review of Optical Sensors for Pesticides. *TrAC Trends in Analytical Chemistry* **2018**, *103*, 1–20, doi:10.1016/j.trac.2018.03.004.
4. Bazot, S.; Bois, P.; Joyeux, C.; Lebeau, T. Mineralization of Diuron [3-(3,4-Dichlorophenyl)-1, 1-Dimethylurea] by Co-Immobilized Arthrobacter Sp. and Delftia Acidovorans. *Biotechnol Lett* **2007**, *29*, 749–754, doi:10.1007/s10529-007-9316-7.
5. Hu, Y. Simultaneous Determination of Phenylurea Herbicides in Yam by Capillary Electrophoresis with Electrochemiluminescence Detection. *Journal of Chromatography B* **2015**, *986–987*, 143–148, doi:10.1016/j.jchromb.2015.02.016.
6. Anh, T.M.; Dzyadevych, S.V.; Van, M.C.; Renault, N.J.; Duc, C.N.; Chovelon, J.-M. Conductometric Tyrosinase Biosensor for the Detection of Diuron, Atrazine and Its Main Metabolites. *Talanta* **2004**, *63*, 365–370, doi:10.1016/j.talanta.2003.11.008.
7. Chen, B.; Wang, X. Combined Approach for Determining Diuron in Sugarcane and Soil: Ultrasound-Assisted Extraction, Carbon Nanotube-Mediated Purification, and Gas Chromatography–Electron Capture Detection. *Journal of Food Science* **2019**, *84*, 2402–2411, doi:10.1111/1750-3841.14752.
8. Wong, A.; De Vasconcelos Lanza, M.R.; Sotomayor, M.D.P.T. Sensor for Diuron Quantitation Based on the P450 Biomimetic Catalyst Nickel(II) 1,4,8,11,15,18,22,25-Octabutoxy-29H,31H-Phthalocyanine. *Journal of Electroanalytical Chemistry* **2013**, *690*, 83–88, doi:10.1016/j.jelechem.2012.11.007.
9. Adeniji, T.M.; Stine, K.J. Nanostructure Modified Electrodes for Electrochemical Detection of Contaminants of Emerging Concern. *Coatings* **2023**, *13*, 381, doi:10.3390/coatings13020381.
10. Ding, L.; Guo, J.; Chen, S.; Wang, Y. Electrochemical Sensing Mechanisms of Neonicotinoid Pesticides and Recent Progress in Utilizing Functional Materials for Electrochemical Detection Platforms. *Talanta* **2024**, *273*, 125937, doi:10.1016/j.talanta.2024.125937.
11. Đurđić, S.; Vlahović, F.; Ognjanović, M.; Gemeiner, P.; Sarakhman, O.; Stanković, V.; Mutić, J.; Stanković, D.; Švorc, Ľ. Nano-Size Cobalt-Doped Cerium Oxide Particles Embedded into Graphitic Carbon Nitride for Enhanced Electrochemical Sensing of Insecticide Fenitrothion in Environmental Samples: An Experimental Study with the Theoretical Elucidation of Redox Events. *Science of The Total Environment* **2024**, *909*, 168483, doi:10.1016/j.scitotenv.2023.168483.
12. Mijajlović, A.; Stanković, V.; Vlahović, F.; Đurđić, S.; Manojlović, D.; Stanković, D. The Cathodically Pretreated Boron-Doped Diamond Electrode as an Environmentally Friendly Electrochemical Tool for the Detection and Monitoring of Mesotrione in Food Samples. *Food Chemistry* **2024**, *447*, 138993, doi:10.1016/j.foodchem.2024.138993.
13. Wang, F.; Zhu, Y.; Qian, L.; Yin, Y.; Yuan, Z.; Dai, Y.; Zhang, T.; Yang, D.; Qiu, F. Lamellar Ti3C2 MXene Composite Decorated with Platinum-Doped MoS2 Nanosheets as Electrochemical Sensing Functional Platform for Highly Sensitive Analysis of

Organophosphorus Pesticides. *Food Chemistry* **2024**, *459*, 140379, doi:10.1016/j.foodchem.2024.140379.
14. Zhang, Q.; Li, P.; Wu, J.; Peng, Y.; Pang, H. Pyridine-Regulated Lamellar Nickel-Based Metal–Organic Framework (Ni-MOF) for Nonenzymatic Electrochemical Glucose Sensor. *Advanced Science* **2023**, *10*, 2304102, doi:10.1002/advs.202304102.
15. Knežević, S.; Ostojić, J.; Ognjanović, M.; Savić, S.; Kovačević, A.; Manojlović, D.; Stanković, V.; Stanković, D. The Environmentally Friendly Approaches Based on the Heterojunction Interface of the LaFeO3/Fe2O3@g-C3N4 Composite for the Disposable and Laboratory Sensing of Triclosan. *Science of The Total Environment* **2023**, *857*, 159250, doi:10.1016/j.scitotenv.2022.159250.
16. Mariyappan, V.; Sundaresan, R.; Chen, S.-M.; Ramachandran, R.; Al-Sehemi, A.G.; Jeevika, A.; Wu, W. Constructing a Novel Electrochemical Sensor for the Detection of Fenitrothion Using Rare-Earth Orthophosphate Incorporated Reduced Graphene Oxide Composite. *Process Safety and Environmental Protection* **2024**, *185*, 726–738, doi:10.1016/j.psep.2024.03.013.
17. Goesmann, H.; Feldmann, C. Nanoparticulate Functional Materials. *Angew Chem Int Ed* **2010**, *49*, 1362–1395, doi:10.1002/anie.200903053.
18. Huang, H.; Zhu, J.-J. The Electrochemical Applications of Rare Earth-Based Nanomaterials. *Analyst* **2019**, *144*, 6789–6811, doi:10.1039/C9AN01562K.
19. Lee, Y.-Y.; Sriram, B.; Wang, S.-F.; Kogularasu, S.; Chang-Chien, G.-P. A Comprehensive Review on Emerging Role of Rare Earth Oxides in Electrochemical Biosensors. *Microchemical Journal* **2023**, *193*, 109140, doi:10.1016/j.microc.2023.109140.
20. Dimesso, L. Pechini Processes: An Alternate Approach of the Sol–Gel Method, Preparation, Properties, and Applications. In *Handbook of Sol-Gel Science and Technology*; Klein, L., Aparicio, M., Jitianu, A., Eds.; Springer International Publishing: Cham, 2016; pp. 1–22 ISBN 978-3-319-19454-7.
21. Huízar-Félix, A.M.; Hernández, T.; De La Parra, S.; Ibarra, J.; Kharisov, B. Sol–Gel Based Pechini Method Synthesis and Characterization of Sm1−xCaxFeO3 Perovskite 0.1≤x≤0.5. *Powder Technology* **2012**, *229*, 290–293, doi:10.1016/j.powtec.2012.06.057.
22. Zaki, T.; Kabel, K.I.; Hassan, H. Using Modified Pechini Method to Synthesize α-Al2O3 Nanoparticles of High Surface Area. *Ceramics International* **2012**, *38*, 4861–4866, doi:10.1016/j.ceramint.2012.02.076.
23. Gaussian 09, Revision A.02.
24. *Horizons of Quantum Chemistry*; Fukui, K., Pullman, B., Eds.; Springer Netherlands: Dordrecht, 1980; ISBN 978-94-009-9029-6.
25. Koch, W.; Holthausen, M.C. *A Chemist's Guide to Density Functional Theory*; 1st ed.; Wiley, 2001; ISBN 978-3-527-30372-4.
26. Zhao, Y.; Truhlar, D.G. The M06 Suite of Density Functionals for Main Group Thermochemistry, Thermochemical Kinetics, Noncovalent Interactions, Excited States, and Transition Elements: Two New Functionals and Systematic Testing of Four M06-Class Functionals and 12 Other Functionals. *Theor Chem Account* **2008**, *120*, 215–241, doi:10.1007/s00214-007-0310-x.
27. Kruse, H.; Grimme, S. A Geometrical Correction for the Inter- and Intra-Molecular Basis Set Superposition Error in Hartree-Fock and Density Functional Theory Calculations for Large Systems. *The Journal of Chemical Physics* **2012**, *136*, 154101, doi:10.1063/1.3700154.

28. Marenich, A.V.; Cramer, C.J.; Truhlar, D.G. Universal Solvation Model Based on Solute Electron Density and on a Continuum Model of the Solvent Defined by the Bulk Dielectric Constant and Atomic Surface Tensions. *J. Phys. Chem. B* **2009**, *113*, 6378–6396, doi:10.1021/jp810292n.
29. Manjunatha, S.; Sunilkumar, A.; Ravikiran, Y.T.; Machappa, T. Effect of Holmium Oxide on Impedance and Dielectric Behavior of Polyaniline–Holmium Oxide Composites. *J Mater Sci: Mater Electron* **2019**, *30*, 10332–10341, doi:10.1007/s10854-019-01371-4.
30. Mortazavi-Derazkola, S.; Zinatloo-Ajabshir, S.; Salavati-Niasari, M. Novel Simple Solvent-Less Preparation, Characterization and Degradation of the Cationic Dye over Holmium Oxide Ceramic Nanostructures. *Ceramics International* **2015**, *41*, 9593–9601, doi:10.1016/j.ceramint.2015.04.021.
31. Faulkner, L.L.; Bard, A.J. *Electrochemical Methods and Applications*; 2nd ed.; Wiley: New Yor, 2001; ISBN 978-0-471-04372-0.
32. Brown, A.P.; Anson, F.C. Electron Transfer Kinetics with Both Reactant and Product Attached to the Electrode Surface. *Journal of Electroanalytical Chemistry and Interfacial Electrochemistry* **1978**, *92*, 133–145, doi:10.1016/S0022-0728(78)80174-0.
33. Temgoua, R.C.T.; Bussy, U.; Alvarez-Dorta, D.; Galland, N.; Hémez, J.; Tonlé, I.K.; Boujtita, M. Simulation of the Environmental Degradation of Diuron (Herbicide) Using Electrochemistry Coupled to High Resolution Mass Spectrometry. *Electrochimica Acta* **2020**, *352*, 136485, doi:10.1016/j.electacta.2020.136485.